

## Two-Point Versus Multipartite Entanglement in Quantum Phase Transitions

Alberto Anfossi<sup>1</sup>, Paolo Giorda<sup>1,2</sup>, Arianna Montorsi<sup>1</sup>, and Fabio Traversa<sup>1</sup>

<sup>1</sup> *Dipartimento di Fisica del Politecnico, C.so Duca degli Abruzzi 24, I-10129 Torino, Italy and*

<sup>2</sup> *Institute for Scientific Interchange (ISI), Villa Gualino, Viale Settimio Severo 65, I-10133 Torino, Italy*

(Dated: July 28, 2005)

We analyze correlations between subsystems for an extended Hubbard model exactly solvable in one dimension, which exhibits a rich structure of quantum phase transitions (QPTs). The  $T = 0$  phase diagram is exactly reproduced by studying singularities of single-site entanglement. It is shown how comparison of the latter quantity and quantum mutual information allows one to recognize whether two-point or shared quantum correlations are responsible for each of the occurring QPTs. The method works in principle for any number  $D$  of degrees of freedom per site. As a by-product, we are providing a benchmark for direct measures of bipartite entanglement; in particular, here we discuss the role of negativity at the transition.

PACS numbers: 03.67.Ud, 71.10.-w

In the past years, the characterization of complex quantum phenomena has received a strong impulse from the recent developments in quantum-information theory. Within such framework, a crucial notion is that of entanglement. Besides being recognized as a fundamental resource for quantum computation and communication tasks [1], it has also been used to better characterize the critical behavior of different many-body quantum systems when some characteristic parameter of the related Hamiltonian is varied; the latter phenomenon being known as quantum phase transition (QPT) [2].

In fact, a deep comprehension of universal properties of QPTs has not been fully reached yet. The peculiarity of using entanglement in this context is that, being a single direct measure of quantum correlations, it should allow for a unified treatment of QPTs; at least, whenever the occurring QPT is to ascribe to the quantum nature of the system, which is always the case at  $T = 0$  since thermal fluctuations are absent.

A first description of the relations between entanglement of one or two spins and QPTs in spin-1/2 chains was given in [3], where it was noticed how derivatives of concurrence show divergencies in correspondence of QPT, with appropriate scaling exponents. The entanglement of blocks of  $L$  spins and its scaling behavior in spin models showing critical behavior was then investigated in [4]. The problem of characterizing the ground state phase diagram of fermionic systems by means of entanglement has been addressed more recently in [5], where it was shown how the study of *single-site entanglement* allows one to reproduce the relevant features of the known (numerical) phase diagram. While this is a promising starting point, it remains to be clarified which quantum correlations are responsible for the occurring QPT: if two-points or shared (multipartite), if short or long ranged. The answer to the above issue would in fact require exhaustive investigation of the entanglement between any two subsystems. In case the subsystems have just two degrees of freedom, concurrence properly quantifies the quantum correlations [6]. A generalization of such quantity to (sub)systems with a higher number of degrees of freedom  $D$  has been proposed, and is known as *negativity* [7]. Also, the total amount of correlations between any two subsystems is captured by *quantum mutual information* [8].

In the following we describe a method based on the comparison of the latter quantities for arguing whether the occurring transition is to ascribe to two-points or multipartite quantum correlations; the method works for arbitrary  $D$ . Our strategy is tested on a one-dimensional extended Hubbard model that was solved [9, 10], exhibiting a rich structure of phase diagram at  $T = 0$ . We show that the phase diagram is exactly reproduced by the singularities of single-site entanglement. We then infer which of the QPTs is originated from a singular behavior of two-point or multipartite entanglement; our results are confirmed by the exact solution.

*Correlations and subsystems.* We are interested in the existing correlations between: *a)* the single site  $i$  and the rest of the system; *b)* the generic site  $i$  and a generic site  $j \neq i$ ; *c)* the generic pair of site  $(i, j)$  (dimer) and the rest of the system. In order to measure the *total correlations* between two generic subsystems  $A$  and  $B$  we use the quantum mutual information [1, 8, 11]. The latter is defined as

$$\mathcal{I}_{AB} = S(\rho_A) + S(\rho_B) - S(\rho_{AB}), \quad (1)$$

where  $\rho_{AB}$ ,  $\rho_A$  and  $\rho_B$  are the system's and subsystems' density matrices, respectively, and  $S(\rho) = -\sum_i \lambda_i \log_2 \lambda_i$  ( $\lambda_i$  being the eigenvalues of  $\rho$ ) is the Von Neumann entropy. In [8, 11] it was shown how  $\mathcal{I}_{AB}$  is a proper measure of all (quantum and classical) correlations between  $A$  and  $B$ . In case  $A$  and  $B$  are single sites, we will refer to the latter as two-point quantum ( $Q2$ ) and classical ( $C2$ ) correlations.

As far as *quantum correlations* are concerned, we consider two different cases. When  $\rho_{AB}$  is a pure state, correlations between  $A$  and  $B$  are purely quantum and are measured by  $S(\rho_A) = S(\rho_B)$ . This happens when  $A$  corresponds to a single site  $i$  (or to the dimer  $(i, j)$ ), and  $B$  corresponds to the remaining sites [12];  $S_i = S(\rho_i)$  (single-site entanglement) accounts for both the localized correlations ( $Q2$ ) and the shared ones ( $QS$  in the following). When we deal instead with the correlations between two generic sites  $(i, j)$ , the density matrix of the global system is the dimer's one:  $\rho_{AB} = \rho_{ij}$ . The latter generally corresponds to a mixed state. Thus, to evaluate the quantum correlations between two generic sites, we need a measure of entanglement for bipartite mixed states.

In general, proposed measures are hard to compute whenever  $D > 2$ , since they require difficult optimization processes. However, there is at least one measure easy to compute[7], the negativity

$$\mathcal{N}(\rho_{AB}) = (\|\rho_{AB}^{TA}\|_1 - 1)/2; \quad (2)$$

where  $\rho_{AB}^{TA}$  is the partial transposition with respect to the subsystem  $A$  applied on  $\rho_{AB}$ , and  $\|O\|_1 \doteq Tr\sqrt{O^\dagger O}$  is the trace norm of the operator  $O$ .  $\rho_{AB}^{TA}$  can have negative eigenvalues  $\mu_i$ , and the negativity can also be expressed as  $\mathcal{N}(\rho_{AB}) = |\sum_i \mu_i|$ . Although negativity is not a perfect measure of entanglement [13], it gives important bounds for quantum information protocols i.e., teleportation capacity and asymptotic distillability. Its role in describing QPTs has not been fully investigated yet.

*Entanglement and QPTs.*  $S_i$  has been proven to be a useful tool in describing QPTs [5]. As already pointed out, to give a better characterization of the latter, one could as well consider quantum correlations between different subsystems. The scheme we propose in this letter is based on the idea of comparing  $S_i$  –not allowing one to distinguish Q2 from QS correlations– with different functionals quantifying instead just two-point correlations. We study  $\mathcal{N}_{i,j}$ , which is at least a lower bound for Q2 correlations, and  $\mathcal{I}_{i,j}$ , which properly captures total (Q2 and C2) correlations. As a first step, the exact phase diagram is obtained analyzing the singularities shown by  $S_i$ ,  $\mathcal{I}_{i,j}$ , and  $\mathcal{N}_{i,j}$ . Successively, a comparison of the singular behavior of  $\mathcal{I}_{i,j}$  with that of  $S_i$  allows one to discriminate whether a QPT is to ascribe to Q2 or QS correlations. In fact, whenever  $S_i$  exhibits a singular behavior due to Q2 correlations, the *same* type of singular behavior should be highlighted as well by  $\mathcal{I}_{i,j}$  (since it also contains Q2 correlations), and possibly by  $\mathcal{N}_{i,j}$ , in case the latter would properly capture them for our model. On the contrary, when the singular behavior of  $S_i$  is to ascribe to QS correlations, the same singular behavior should not be displayed either by  $\mathcal{I}_{i,j}$  or by  $\mathcal{N}_{i,j}$ , since both measures regard only two-point correlations.

*The bond-charge extended Hubbard model.* The model we deal with is described by the following Hamiltonian:

$$H_{BC} = u \sum_i n_{i\uparrow} n_{i\downarrow} - \sum_{\langle i,j \rangle > \sigma} [1 - x(n_{i\bar{\sigma}} + n_{j\bar{\sigma}})] c_{i\sigma}^\dagger c_{j\sigma}, \quad (3)$$

where  $c_{i\sigma}^\dagger, c_{i\sigma}$  are fermionic creation and annihilation operators on a one-dimensional chain of length  $L$ ;  $\sigma = \uparrow, \downarrow$  is the spin label,  $\bar{\sigma}$  denotes its opposite,  $n_{j\sigma} = c_{j\sigma}^\dagger c_{j\sigma}$  is the spin  $\sigma$  electron charge, and  $\langle i, j \rangle$  stands for neighboring sites;  $u$  and  $x$  ( $0 \leq x \leq 1$ ) are the (dimensionless) on-site Coulomb repulsion and bond-charge interaction parameters.

The model is considered here at  $x = 1$ , in which case the number of doubly occupied sites becomes a conserved quantity. The exact eigenstates of  $H_{BC}(x = 1)$  are obtained in [9, 10, 14]; the ground-state phase diagram is shown in the left part of Fig. 1. The latter presents various QPTs driven by parameters  $u$  and average number of electrons per site (filling)  $n$ . The charge-gapped phase IV is insulating and all sites are

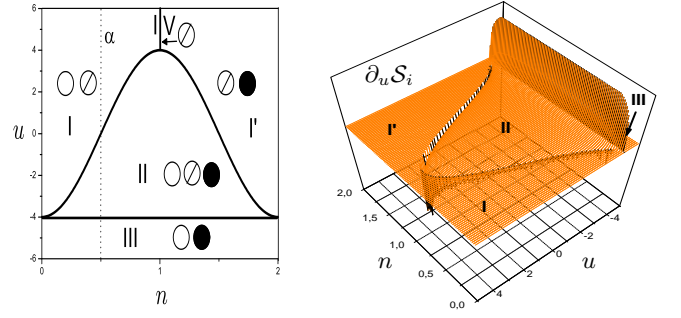


FIG. 1: Left: Ground-state phase diagram. Empty, slashed and full dots stay for empty, singly and doubly occupied sites. Right:  $\partial_u S_i$ .

singly occupied; phases  $I$ ,  $I'$ , and  $II$  fall in the Tomonaga-Luttinger class (neither spin nor charge gap); they are characterized by the presence of singly and empty sites (phase  $I$ ), singly and doubly occupied sites (phase  $I'$ ), both of which have dominant charge-charge correlations, and all types of sites (phase  $II$ ) with superconducting correlations and off-diagonal long range order (ODLRO). The latter characterizes also phase  $III$ , where sites are empty or doubly occupied.

The model's energy spectrum is fully independent of spin orientation [9]: any sequence of spins in the chain cannot be altered by the Hamiltonian, which, in fact, acts on a Hilbert space that at each site  $i$  has  $D_i = 3$ , and is spanned by the states  $|0\rangle_i$  (empty),  $|\phi\rangle_i$  (singly occupied), and  $|2\rangle_i$  (doubly occupied). The physics of the system is essentially that of  $N_s = \sum_i c_i^\dagger c_i$  spinless fermions and  $N_d$  bosons, with eigenstates given by

$$|\psi(N_s, N_d)\rangle = \mathcal{N}(\eta^\dagger)^{N_d} a_0^\dagger \cdots a_{N_s-1}^\dagger |vac\rangle. \quad (4)$$

Here  $\mathcal{N} = [(L - N_s - N_d)! / (L - N_s)! N_d!]^{1/2}$  is a normalization factor;  $a_j^\dagger$  is the Fourier transform of the spinless fermion operator  $c_j^\dagger$ ,  $a_j^\dagger = \sum_q \frac{1}{\sqrt{L}} \exp(i\frac{\pi}{L}jq) c_q^\dagger$ , with  $j = 0, \dots, N_s - 1$ ; moreover  $\eta^\dagger = \sum_{i=1}^L \eta_i^\dagger$  is also known as the eta operator, and creates doubly occupied sites from empty ones ( $\eta_i^\dagger |0\rangle_i = |2\rangle_i$ );  $|vac\rangle$  is the electron vacuum.  $(\eta^\dagger)^k |vac\rangle$  is known to carry ODLRO and multipartite entanglement [15]. At fixed filling  $n = (N_s + 2N_d)/L$ , the actual value of  $N_s$  in (4) is chosen to minimize the corresponding eigenvalue  $E(N_s, N_d) = -2\frac{L}{\pi} \sin(\pi\frac{N_s}{L}) + uN_d$ .

The system density matrix in the ground state is defined by  $\rho \doteq |\psi(N_s, N_d)\rangle \langle \psi(N_s, N_d)|$ . Results of the calculation for the single-site  $\rho_i$  and the dimer  $\rho_{ij}$  reduced density matrices are reported below. With respect to the basis  $|0\rangle, |\phi\rangle, |2\rangle$ ,  $\rho_i = \text{diag}\{1 - n_s - n_d, n_s, n_d\}$  with  $n_\alpha \doteq \frac{N_\alpha}{L}$  ( $\alpha = s, d$ ). Whereas with respect to the basis  $|00\rangle, |0\phi\rangle, |\phi 0\rangle, |\phi\phi\rangle, |\phi 2\rangle, |2\phi\rangle, |02\rangle, |20\rangle, |22\rangle$ ,

$$\rho_{ij} = \begin{pmatrix} D_1 & 0 & 0 & 0 & 0 & 0 & 0 & 0 & 0 \\ 0 & O_1 & O_2 & 0 & 0 & 0 & 0 & 0 & 0 \\ 0 & O_2^* & O_1 & 0 & 0 & 0 & 0 & 0 & 0 \\ 0 & 0 & 0 & D_2 & 0 & 0 & 0 & 0 & 0 \\ 0 & 0 & 0 & 0 & P_1 & P_2 & 0 & 0 & 0 \\ 0 & 0 & 0 & 0 & P_2^* & P_1 & 0 & 0 & 0 \\ 0 & 0 & 0 & 0 & 0 & 0 & Q & Q & 0 \\ 0 & 0 & 0 & 0 & 0 & 0 & Q & Q & 0 \\ 0 & 0 & 0 & 0 & 0 & 0 & 0 & 0 & D_3 \end{pmatrix} \quad (5)$$

Here, assuming  $\epsilon = 1/L$ ,

$$\begin{aligned} D_1 &= P_{ij} \frac{(\delta_s - n_d)(\delta_s - n_d - \epsilon)}{\delta_s(\delta_s - \epsilon)} & O_2 &= C_{ij} \frac{\delta_s - n_d}{\delta_s} \\ D_2 &= P_{ij} + 1 - 2\delta_s & P_1 &= \frac{n_d}{\delta_s} (\delta_s - P_{ij}) \\ D_3 &= \frac{n_d(n_d - \epsilon)}{\delta_s(\delta_s - \epsilon)} P_{ij} & P_2 &= \frac{n_d}{\delta_s} C_{ij} \\ O_1 &= (\delta_s - P_{ij}) \left( \frac{\delta_s - n_d}{\delta_s} \right) & Q &= \frac{n_d(\delta_s - n_d)}{\delta_s(\delta_s - \epsilon)} P_{ij} \end{aligned}$$

with  $P_{ij} = \delta_s^2 - |C_{ij}|^2$ ,  $\delta_s = 1 - n_s$ ,  $|C_{ij}| = \epsilon \frac{\sin(n_s \pi |i-j|)}{\sin(\pi \epsilon |i-j|)}$ . In the thermodynamic limit  $\epsilon \rightarrow 0$ ,  $n_\alpha$  finite, the above results may also be derived from [10].

*Results.* As a preliminary observation let us notice that in phases  $I$ ,  $I'$  and  $III$  (see Fig. 1, left side) the dimension of on-site vector space reduces to two, meaning that in these cases  $\mathcal{N}_{i,j}$  should reproduce results evaluated through concurrence. This happens to be the case; in particular, in phase  $III$   $\mathcal{N}_{i,j}$  (and the concurrence) are vanishing  $\forall |i-j|$ , whereas  $\mathcal{I}_{i,j}$  is equal to  $n(2-n)/2$ , which is related to the value of the ODLRO parameter, in agreement with [15].

We also observe that whenever  $C_{i,j}$  is zero (for instance, phases  $III$  and  $IV$ ) the two-site density matrix is independent of the sites  $i$  and  $j$ . In the insulating phase  $IV$  this happens because the state is a tensor product of identical single-site states, and all correlations are identically zero. On the contrary, in phase  $III$ , since  $Q \neq 0$ , the surviving two-point quantum correlations are range independent. In such cases it may be useful to introduce global (*i.e.* sums over all sites) quantities instead of local ones, since it may happen that a correlation is locally vanishing but globally relevant; also finite size corrections ( $\epsilon$ ) have to be considered. For instance, it turns out that in so doing in phase  $III$  the total negativity becomes nonvanishing  $\sum_{j \neq i} \mathcal{N}_{i,j} = n(2-n)/[(2-n)^2 + n^2]$ .

We now turn to discuss what happens at QPTs by studying the behavior of  $\mathcal{S}_i$ ,  $\mathcal{I}_{i,j}$ ,  $\mathcal{N}_{i,j}$ . As mentioned, each of the observed measures of correlations keeps track of the underlying transitions, exhibiting a singular behavior at the transition points. The latter can be characterized by the analysis of the partial derivatives of each measure. As an example, in the right part of Fig. 1 we plot  $\partial_u \mathcal{S}_i$ . Noticeably, the divergencies in the derivative are in perfect correspondence with the parameter's values at which the various QPTs occur, aside from transitions  $I, I' \rightarrow IV$  that must be revealed by  $\partial_n \mathcal{S}_i$ . The systematic analysis of the behavior of the various derivatives at each QPT is carried on in Table I. We first consider

	$\partial_x \mathcal{S}_i$	$\partial_x \mathcal{I}_{i,j}$	$\partial_x \mathcal{N}_{i,j}$	ent
$I, I' \rightarrow IV(x=n)$	$\log  n_c - n $	FD	0	Multi
$II \rightarrow I, I'(x=u)$	$\log(u_c - u)$	FD	FD	Multi
$II \rightarrow I, I'(x=n)$	$\log  n - n_c $	FD	FD	Multi
$II \rightarrow III(x=u)$	$1/\sqrt{u - u_c}$	$1/\sqrt{u - u_c}$	FD	Two
$II \rightarrow IV(x=u)$	$1/\sqrt{u_c - u}$	$1/\sqrt{u_c - u}$	FD	Two

TABLE I: Behavior of the evaluated partial derivatives at critical points for the various QPTs (left column): FD is finite discontinuity, “multi” refers to multipartite, and “two” refers to two-point.

$\partial_x \mathcal{S}_i$ ,  $x = n, u$ ; it exhibits two different kinds of divergencies: logarithmic for transitions  $I, I' \rightarrow IV$  and  $II \rightarrow I, I'$ ; algebraic for transitions  $II \rightarrow III$  and  $II \rightarrow IV$ , with exponent  $\nu = 1/2$ . The latter turns out to correspond to the shift exponent as extracted from finite size analysis [16].

In Tab. I we also report the behavior of  $\partial_x \mathcal{I}_{i,j}$  and  $\partial_x \mathcal{N}_{i,j}$  at QPTs. As described in the paragraph *Entanglement and QPTs*, the comparison of the three quantities can be used to understand whether bipartite or multipartite entanglement is relevant to the various transitions. In fact, all transitions corresponding to a (logarithmic) divergence in  $\partial_x \mathcal{S}_i$  are not seen as divergencies either in  $\partial_x \mathcal{I}_{i,j}$  or in  $\partial_x \mathcal{N}_{i,j}$ . In such cases, we infer that the transitions are to ascribe to  $QS$  correlations; this is also in agreement with the fact in some of these transitions ( $II \rightarrow I, I'$ ) the component of the ground state given by the eta pairs (which carry multipartite entanglement and ODLRO) disappears. On the contrary, whenever the divergent behavior exhibited by  $\partial_x \mathcal{S}_i$  is also displayed by  $\partial_x \mathcal{I}_{i,j}$ , as seen for the two transitions  $II \rightarrow III$  and  $II \rightarrow IV$ , this is to be interpreted as a signal of the role of  $Q2$  correlations in the QPT.

Different from what happens for the first two quantities reported in Table I, we can check on the third column that  $\partial_x \mathcal{N}_{i,j}$  never does display the same singular behavior as  $\partial_x \mathcal{S}_i$ . In particular, this happens in correspondence of the transitions driven by two-point correlations,  $II \rightarrow III$  and  $II \rightarrow IV$ , suggesting that  $\mathcal{N}_{i,j}$  is just a lower bound for  $Q2$  correlations also for the present model. Apart from this fact, the behavior of  $\mathcal{N}_{i,j}$  for various values of  $|i-j|$  supports once more the idea that the transitions in question have to be ascribed to two-point correlations. As an example, we report in the top left part of Fig. 2  $\mathcal{N}_{i,j}$  for the case  $n = 0.5$ ; the transition  $II \rightarrow III$  takes place at  $u_c = -4$ . As  $u$  gets close to  $u_c$  two-point quantum correlations begin to spread along the chain; this is shown by the non zero value of  $\mathcal{N}_{i,j}$  for an increasing number of pairs of sites whose distance  $|i-j|$  grows up to  $\infty$  as  $u \rightarrow u_c$ . This is a clear indication of diverging correlation length originated from  $Q2$  correlations at critical point. One could expect that again the total negativity is the right quantity to display a critical behavior, in agreement with similar conclusions about concurrence [17] in spin-1/2 systems. Moreover, the value at which  $\mathcal{N}_{i,j}$  reaches its maximum gets closer to  $u_c$  by increasing  $|i-j|$ , indicating its possible scaling behavior. The same qualitative behavior of maximum is

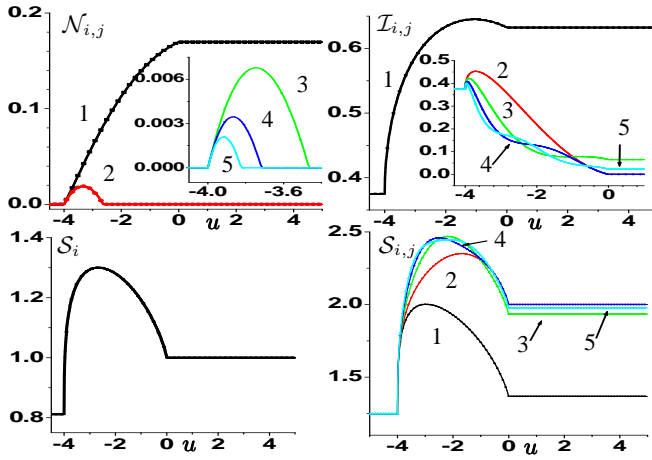


FIG. 2: Plots of  $\mathcal{N}_{i,j}$ ,  $\mathcal{I}_{i,j}$ ,  $S_i$  and  $\mathcal{S}_{i,j}$  ( $|i-j| = 1, \dots, 5$ ) for the section  $n = 0.5$  (line  $\alpha$  in Fig. 1)

observed for  $\mathcal{I}_{i,j}$  (top right part of figure), even though such a quantity is, in general, different from zero also away from the critical point, suggesting once more that the quantum mutual information in the vicinity of the transition captures the divergent behavior of just the  $Q2$  correlations. We finally analyze in Fig. 2  $\mathcal{S}_{i,j} = \mathcal{S}(\rho_{i,j})$ , which describes all quantum correlations between the dimer  $i, j$  and the rest of the system. Interestingly,  $\mathcal{S}_{i,j}$  has for all  $i, j$  the same qualitative behavior of  $S_i$  at critical points. Such a feature is confirmed by our calculations in correspondence of all QPTs. This is expected within our scheme, since  $S_i$  and  $\mathcal{S}_{i,j}$  both describe the same correlations,  $Q2$  and  $QS$ .

**Conclusions.** We have studied the behavior of different measures of correlations in correspondence of QPTs for a solvable model of correlated electrons on a chain, displaying different kinds of metal-insulator-superconductor transitions. As a general output of our work, the role of quantum mutual information in the investigation of QPTs has been recognized. In particular, the comparison of singularities of the latter quan-

tity with singularities of single-site entanglement allows one to distinguish at each QPT the contribution of bipartite from that of multipartite entanglement. At the same time, whenever a contribution from two-point quantum correlations is spotted, this can be used to test direct measures of bipartite entanglement. As an example, we tested the negativity, finding that in this case it does not capture all of the two-point quantum correlations, though it shows evidence of a diverging correlation length and interesting scaling behavior in the vicinity of the transitions ascribed to two-point correlations. The study of scaling properties of the proposed measures of entanglement and of total negativity [16] need to be further investigated.

- 
- [1] M.A. Nielsen and I.L. Chuang, *Quantum Computation and Quantum Information* (Cambridge University Press, Cambridge, UK 2000).
  - [2] S.Sachdev, *Quantum Phase Transitions* (Cambridge University Press, Cambridge, UK 2000).
  - [3] A. Osterloh et al., Nature (London) **416**, 608 (2002); T.J. Osborne and M.A. Nielsen, Phys. Rev. A **66**, 032110 (2002).
  - [4] J. I. Latorre, E. Rico, G. Vidal, Quantum Inf. Comput., **4** 48 (2004); G. Vidal et al., Phys. Rev. Lett. **90**, 227902 (2003).
  - [5] S. Gu et al., Phys. Rev. Lett. **93**, 086402 (2004).
  - [6] W. K. Wootters, Phys. Rev. Lett. **80**, 2245 (1998).
  - [7] G. Vidal and R. F. Werner Phys. Rev. A **65**, 032314 (2002).
  - [8] B. Groisman, S. Popescu, and A. Winter, quant-ph/0410091.
  - [9] L. Arrachea, and A.A. Aligia, Phys. Rev. Lett. **73**, 2240 (1994).
  - [10] A. Schadschneider, Phys. Rev. B **51**, 10386 (1995).
  - [11] V. Vedral, Rev. Mod. Phys. **74**, 197-234 (2002).
  - [12] P. Zanardi, Phys. Rev. A **65**, 042101 (2002); H. Fan, and S. Lloyd, J. Phys. A **38**, 5285 (2005).
  - [13] S. Lee et al., Phys. Rev. A **68**, 062304 (2003).
  - [14] F. Dolcini, and A. Montorsi, Phys. Rev. B **66**, 075112 (2002).
  - [15] V. Vedral, New J. Phys. **6**, 102 (2004).
  - [16] A. Anfossi, P. Giorda, and A. Montorsi (to be published).
  - [17] Z. Sun et al., Commun. Theor. Phys. **43**, 1033 (2005).